# Accurate Evaluation of Aberration for Probe-Forming System and Influence of Aberration on High-Resolution STEM image

IOP Conf. Series: Journal of Physics: Conf. Series **902** (2017) 012012 doi:10.1088/1742-6596/902/1/012012

# Accurate Evaluation of Aberration for Probe-Forming System and Influence of Aberration on High-Resolution STEM image

**Hidetaka Sawada[1,2,3], Fumio Hosokawa[4] and Angus I. Kirkland[1,2]**

[1]ePSIC: Electron Physical Sciences Imaging Centre, Diamond Light Source Ltd, Didcot, Oxford, OX11 0DE, UK
[2]Department of Materials, University of Oxford, Parks Road, Oxford OX1 3PH, UK
[3]JEOL UK Ltd., Silver Court Watchmead Welwyn Garden City, Herts., AL7 1LT, UK
[4]BioNet Laboratory Inc., 2-3-28 Nishiki-chou, Tachikawa, Tokyo, 190-0022 Japan

E-mail: hide.sawada@materials.ox.ac.uk

**Abstract.** The influence of residual three-fold astigmatism on high-resolution STEM imaging of graphene has been investigated. The aberration was measured by the segmented Ronchigram auto-correlation function method using the graphene lattice. In the presence of residual three-fold astigmatism the graphene lattice showed a lower three-fold rotational symmetry where three C atoms in the six membered ring had a higher intensity.

## 1. Introduction

Aberration corrected instruments are commonly used to obtain high-resolution imaging in both STEM and TEM [1,2], and single atoms of light elements including boron, carbon, nitrogen, and oxygen can now be imaged in two-dimensional materials. For visualization of single atoms in two-dimensional materials, residual aberrations affect the image quality in STEM by altering the probe shape. Automated measurement and adjustment of the aberrations in the probe-forming system can be achieved using pairs of over and under focus images of nm sized metal particles supported on a carbon film by deconvolution of probe shapes using a Gaussian focus image [1]. Alternatively, the Ronchigram can be used to measure aberrations with beam induced image shifts [2] and segmentation of Ronchigrams recorded from amorphous films [3] or lattices [4, 5]. However, even after auto-adjustment [1-3], residual aberration can be introduced by the hysteresis in the objective lens, specimen charging and other factors. During high-resolution image observation it is possible to manually correct first-order defocus and two-fold astigmatism to optimize these aberration. Second-order axial coma can also generally be corrected manually by observing the Rongchigram. However, second-order three-fold stigmatism is not easy to correct manually by observing a high-resolution image or a Ronchigram. Nonetheless, three-fold astigmatism can introduce artifacts in high-resolution images, potentially leading to incorrect interpretation for quantitative analysis. We have developed a method to measure this aberration using a two-dimensional lattice [6]. Importantly using this method, a high-resolution image of a two-dimensional material and the aberration measurement can be performed with the same probe-forming condition and the same specimen. It is useful to understand the influence of this aberration directly on high-resolution STEM images and hence we have evaluated its effects using STEM images of monolayer graphene.

## 2. Aberration measurement and high-resolution observation of graphene

Ronchigrams from an amorphous film (Fig.1(a)) and from monolayer graphene ((Fig.1(b)) were recorded using a JEM-ARM300F equipped with a STEM spherical aberration corrector at an accelerating voltage of 80 kV. The Ronchigram of graphene was divided into local angular areas and the lateral magnification change for each segment was measured using the auto-correlation function (Fig 1(c)). Aberration coefficients were measured from the auto-correlation patterns and the values of the aberration coefficients up to 3rd order are listed in Table 1. Figure 1(d) shows a high-resolution low-angle-annular-dark-field (LAADF) STEM image of a monolayer graphene sample. The C-C spacing at 142 pm are clearly resolved and the intensity of all carbon atoms in the 6-membered rings are equivalent, as shown in the intensity line profile in Fig. 1(e).

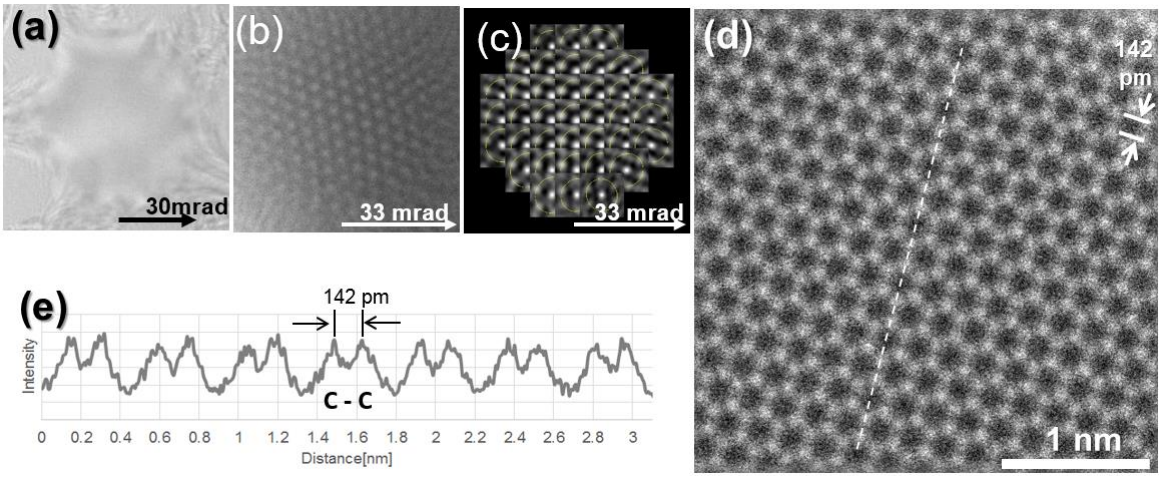


**Figure 1.** (a) Ronchigrams obtained from an amorphous film at 80kV with a camera length of 80 cm. (b) Experimental Ronchigram recorded from monolayer graphene. (c) Local area auto-correlation patterns from an array of 37 sub-areas. (d) LAADF STEM image of graphene at an accelerating voltage of 80kV with a convergence semi-angle of 25 mrad with 23 pA. 30 frames of 512 x 512 pixels were averaged to produce the image in (e) with a dwell time of 4 μs/pixel for each frame. (e) Intensity line profile from the dotted line in Fig.1(d) with 10 pixel width.

**Table 1.** Aberration coefficients up to third order from the measurements shown in Figure 1(c). Values in brackets correspond to errors in the measurement values.

| **Aberration** | **Amplitude** | **Azimuth** |
|---|---|---|
| O2: Defocus | –51.852 [nm] (0.11 [nm]) | |
| A2: Two-fold stigmatism | 0.276 [nm] (0.09 [nm]) | 84.34º (7.57 %) |
| P3: Axial Coma | 17.598 [nm] (3.46 [nm]) | –144.39º (3.67 %) |
| A3: Three-fold astigmatism | 16.436 [nm] (2.42 [nm]) | –0.19º (2.15 %) |
| A4: Four-fold astigmatism | 0.173 [μm] (0.08 [μm]) | 29.66º (7.33 %) |
| Q4: Star aberration | 0.654 [μm] (0.16 [μm]) | 53.16º (4.57 %) |
| O4: 3rd order spherical aberration | 0.833 [μm] (0.15 [μm]) | |

## 3. High-resolution STEM image with a three-fold astigmatism

Figures 2(a) and 2(d) show Ronchigrams recorded at 80 kV with a camera length of 80 cm from monolayer graphene with a focused STEM probe in which a three-fold astigmatism was intentionally introduced. The Ronchigram was segmented into 21 local angular areas and auto-correlation patterns were calculated from each area, shown in Figures 2(b) and 2(e). Table 2 lists the aberration coefficients up to third order calculated from the oval fits, showing a large value of the three-fold astigmatism. Figures 2(c) and 2(f) show the calculated phase using the measured aberrations in Table 2. In the phase

map the three fold symmetry due to A3 is dominant and the polarity of the three-fold astigmatism is opposite in Figs.2(c) and 2(f).

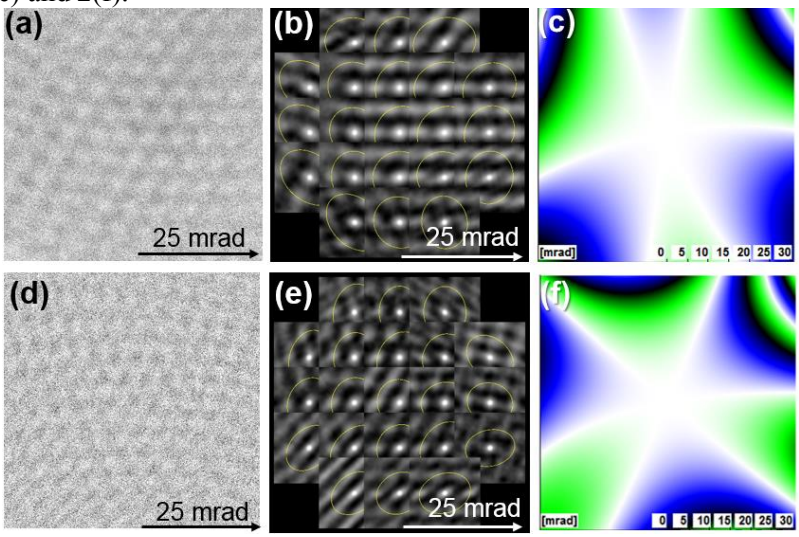


**Figure 2**. (a) and (d) Experimental Ronchigrams recorded from monolayer graphene with three-fold astigmatism. The Ronchigrams are shown up to 25 mrad. (b) and (e) Local area auto-correlation functions patterns calculated from the Ronchigrams in (a) and (d) with corresponding oval fits. (c) and (f) Calculated phases using the measured aberrations from (b) and (e), respectively (Table 2). White to black corresponds to π. Blue and light green show the opposite sign of the phase. Defocus and two-fold astigmatism are set to zero for the phase simulation, since first-order aberrations were adjusted during high-resolution STEM observation.

**Table 2.** Measured aberration coefficients from Fig. 2(b) and in Fig. 2(e).

| Aberration | Amplitude in Fig.2(b) | Azimuth | Amplitude in Fig.2(e) | Azimuth |
|---|---|---|---|---|
| O2 | –52.039 [nm] (0.47 [nm]) | | –59.455 [nm] (0.52 [nm]) | |
| A2 | 1.381 [nm] (0.50 [nm]) | –43.47º (5.41 %) | 4.335 [nm] (0.56 [nm]) | –47.46º (1.41 %) |
| P3 | 80.055 [nm] (11.48 [nm]) | 108.91º (2.45 %) | 80.113 [nm] (16.73 [nm]) | 114.56º (2.08 %) |
| A3 | **113.655** [nm] (11.63 [nm]) | **38.32º** (1.29 %) | **191.105** [nm] (11.19 [nm]) | **–17.63º** (0.70 %) |
| A4: | 0.141 [μm] (0.40 [μm]) | –35.25º (50.86 %) | 1.180 [μm] (0.55 [μm]) | – 35.25º (1.32 %) |
| Q4 | 1.419 [μm] (0.76 [μm]) | –4.02º (8.02 %) | 2.407 [μm] (0.73 [μm]) | – 4.02º (5.94 %) |
| O4 | 1.412 [μm] (0.59 [μm]) | | –0.985 [μm] (0.76 [μm]) | |

STEM images of monolayer graphene in Figs.3(a) and (e) were recorded with a three-fold astigmatism (Table 2). Three atomic positions show brighter intensity within the 6-member C rings (Fig.3(a)); the carbon at position "A" is brighter than that at position "B", although all atomic position corresponds to a single carbon atom (Fig. 3(b)). Figs. 3(c) and (d) show a simulated STEM LAADF image of monolayer graphene and the corresponding simulated probe with A3=113.655 nm at 38.32º [7]. The atomic position at "A" is also brighter than at "B" in these simulations. However, the STEM image for the opposite polarity of a A3 (191.105 nm at ‑17.63º) (Fig.3(e)) shows that the atomic position "B" is brighter than that at "A" in both the simulated and experimental images (Figs.3(f) and (g)). Importantly, for both cases the 6-fold rotational symmetry of graphene is lowered to a 3-fold rotational symmetry. These results clearly demonstrate that aberration introduce significant artefacts in quantitative interpretation for STEM imaging.

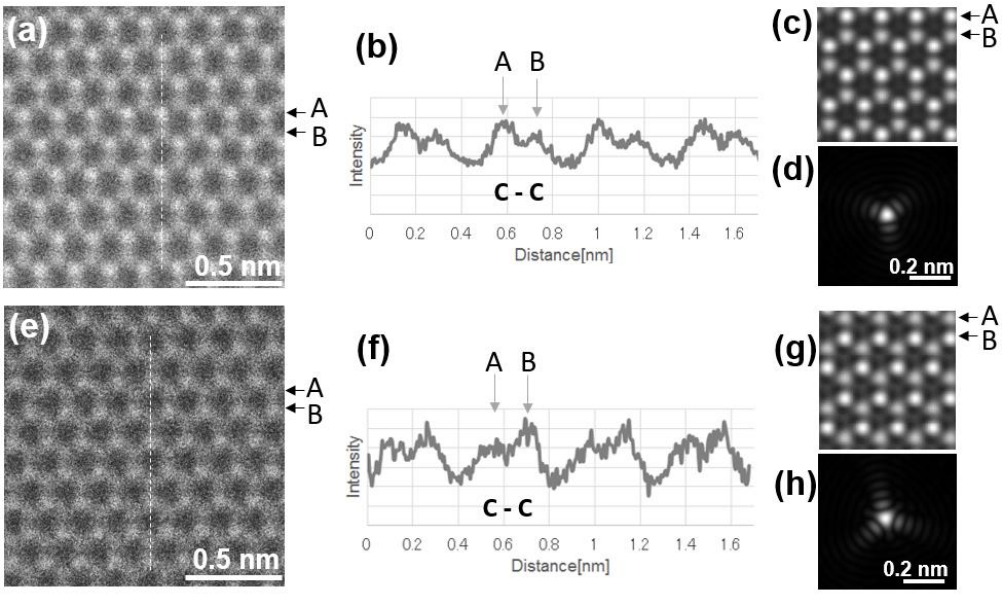


**Figure 3**. (a) Experimental LAADF STEM image of graphene at an accelerating voltage of 80kV with a convergence semi-angle of 25mrad and a beam current of 23 pA with an A3 value corresponding to Fig.2(a). Ten frames were averaged with a dwell time of 20 μs/pixel for each frame. (b) Intensity line profile from the white dotted line with a 10 pixel width from Fig.3(a). (c) Simulated LAADF image with A3=113.655 nm at 38.32°. (d) Simulated probe for the same value of A3 as in (c). (e) Experimental LAADF STEM image of graphene with an A3 value corresponding to Fig.2(d). Ten frames were averaged with a dwell time of 20 μs/pixel for each frame. (f) Intensity line profile from the white dotted line with a 10 pixel width from Fig.3(e). (g) Simulated LAADF image with A3=191.105 nm at -17.63°. (f) Simulated probe for the same value of A3 as in (g)

## 4. Conclusion

Three-fold astigmatism was accurately measured using the segmented Ronchigram auto-correlation function patterns recorded from a graphene lattice. LAADF images of a monolayer graphene in the presence of this aberration showed a lower three-fold rotational symmetry. Moreover, when the azimuth of a residual three-fold aberration was rotated, the positon of the atoms having stronger intensity were changed.

.

## References

[1] Haider M., Uhlemann S, and Zach J 2000 *Ultramicroscopy* **81** 163-175.
[2] Dellby N, Krivanek, O L, Nellist P D, Batson, P E and Lupini A. R 2001 *J. Electron Microsc*., **50**, 177-185.
[3] Sawada H, Sannomiya T, Hosokawa F, Nakamichi T, Kaneyama, Tomita T, Kondo Y, Tanaka T, Oshima Y, Tanishiro Y, and Takayanagi K. 2008 *Ultramicroscopy* **108** 1467-1475.
[4] Lupini A R and Pennycook S J 2008 *J. Electron Microsc.,* **57** 195-201.
[5] Yamazaki T, Kotaka Y, Kikuchi Y and Watanabe, K 2006 *Ultramicroscopy,* **106**, 153-163.
[6] Sawada H, Allen S.C, Wang S, Warner J H, and Kirkland A I 2017 *Ultramicroscopy,* accepted.
[7] elbis:Electron-Beam Image Simulator for Aberration Corrected TEM/ STEM and Diffractions (http://www.bio-net.co.jp/SP-elbis_e/index.html)